BAM
Bundesanstalt für Materialforschung und -prüfung

Industrial Computed Radiography with storage phosphor imaging plates – results of a classification of the system Dürr HD-CR 35 NDT Plus scanner using HD-IP Plus imaging plates (HD-IP^{+})

BAM reference	BAM 8.3 / 7648a
Report date	May 6th 2014
Customer	Dürr NDT GmbH & Co. KG Höpfigheimer Straße 22 D-74321 Bietigheim-Bissingen Germany
Reference	Contract No. BAM ZBA-0001-2006-Dürr
Test samples	"HD-CR 35 NDT Plus" scanner, serial number D238825008, 6 imaging plates "HD-IP Plus", 10x24 cm², charge number 94172935-N1002
Receipt of samples	September 25th 2013
Test date	December 2013
Test location	BAM Berlin
Test procedure	Measurements for system classification of the CR system HD-CR 35 NDT Plus scanner and HD-IP^{+} imaging plates, evaluation of image quality, CEN speed, basic spatial resolution and IP system classes depending on exposure dose according to the standards EN 14784-1, ISO 16371-1 and ASTM E 2446 and E 2445
Test specifications	according to EN 14784-1, ISO 16371-1 and ASTM E 2445 and E 2446

TEST REPORT

This test report consists of page 1 to 15 and enclosures 14 figures.

Aim of testing

The primary aim of this investigation was the evaluation and classification of the above mentioned CR system according to table 1 in EN 14784-1. The normalized signal-to-noise ratios were measured according to section 6.1.1 (step exposure method) in EN 14784-1, the minimum read-out intensities I_{IPx} were calculated according to 6.2 and the image unsharpness parameters were determined according to 6.3 (MTF-method and duplex wire method) to estimate the maximum basic spatial resolution SR_{max}. The CEN speeds S_{CEN} were determined for all IP system classes. All other tests described in section 6.4.1 up to 6.4.5 and annex B of EN 14784-1 have been carried out based on a CR test phantom (S/N D000004 from Kowotest GmbH).
This test report gives only references to EN 14784-1 for simplicity since ASTM E 2445 and 2446 have identical requirements, but they are structured in different sections compared to the EN standard. ISO 16371-1 is identical to EN 14784-1.

Summary of test results

The measurements according to EN 14784-1, ISO 16371-1 and ASTM E 2446 are summarized in the following CR system classification of the above CR system of Dürr NDT GmbH & Co. KG:

ASTM system class	CEN system class	minimum normalized SNR_{IPx}	minimum dose K_S / mGy	CEN / ISO speed $S_{CEN} = S_{ISO}$	minimum linearized intensity I_{IPx}
IP special / 40	IP1/40	130	8,99	100	13050
	IP2/40	117	6,35	160	9200
	IP3/40	78	2,23	500	3250
IP I / 40	IP4/40	65	1,58	640	2300
IP II / 40	IP5/40	52	1,11	1000	1650
IP III / 40	IP6/40	43	0,87	1250	1300

Table 1: CR system classification for the HD-CR 35 NDT Plus scanner and HD-IP$^+$ imaging plates (pixel size: 15.5 µm). Film plastic bags have been used for exposure without lead screens.

System set-up for classification

All investigations reported in this test have been carried out with the scanner set-up shown in fig.1. The raw data have been acquired with system software Vistascanconfig.exe, which is installed by default, when the user installs software for the scanner HD-CR 35 NDT Plus on a PC. This is not always necessary, because the scanner can be operated from the built-in touch panel using the internal embedded Linux computer (firmware version 1.2.1.1870) to store images on a SD card or transfer it via Ethernet cable or WLAN to a server. By starting the programme “Vistascanconfig.exe” (Version 7.1.0.12122 was used for certification) the scan mode “BAM Certified Mode (15/15/30)” as shown in fig. 1 was selected as scanning mode under the tab “Scan Modes”. Following this, the button “Read Image” can be pressed at the tab “Test” and a new window “Scan preview” is opened at the Windows desktop, showing “Device ready”. After pressing the “Start Scan” button 4 green indicators on the touch panel of the scanner should light to indicate that the scanner is ready for scanning. The scan mode shown in fig. 1 scans at 2114 rotations per minute with a shift of 31 µm per rotation in slow scan mode. This gives a scanning speed of 65.5 mm/minute of the imaging plate. An IP of size 24x10 cm² was scanned and all data are transferred to the PC within 2 min. A data file of 190 MBytes is created with a pixel size of 15.5 µm in the sub-dir “C:\Duerr\Images\” as “*.PNG” file. These “*.PNG” image files (format according to Portable Network Graphics standard, see RFC 2083, 1997) were finally loaded into the BAM image analysis tool “Isee!” (version 1.11.1), see http://dir.bam.de/ic.html). The original image raw data (gv_{raw}) sent by the HD-CR 35 NDT Plus scanner are dose proportional and have full 16

bit resolution. All analysis according to EN 14784-1 have to be based on a linearized signal intensity scale (I_{meas}), starting from Zero at Zero dose exposure. No conversion of these raw grey values was needed to fulfil this condition, because the digitized raw data are directly proportional to the photo stimulated luminescence measured with the internal photo multiplier of this scanner.

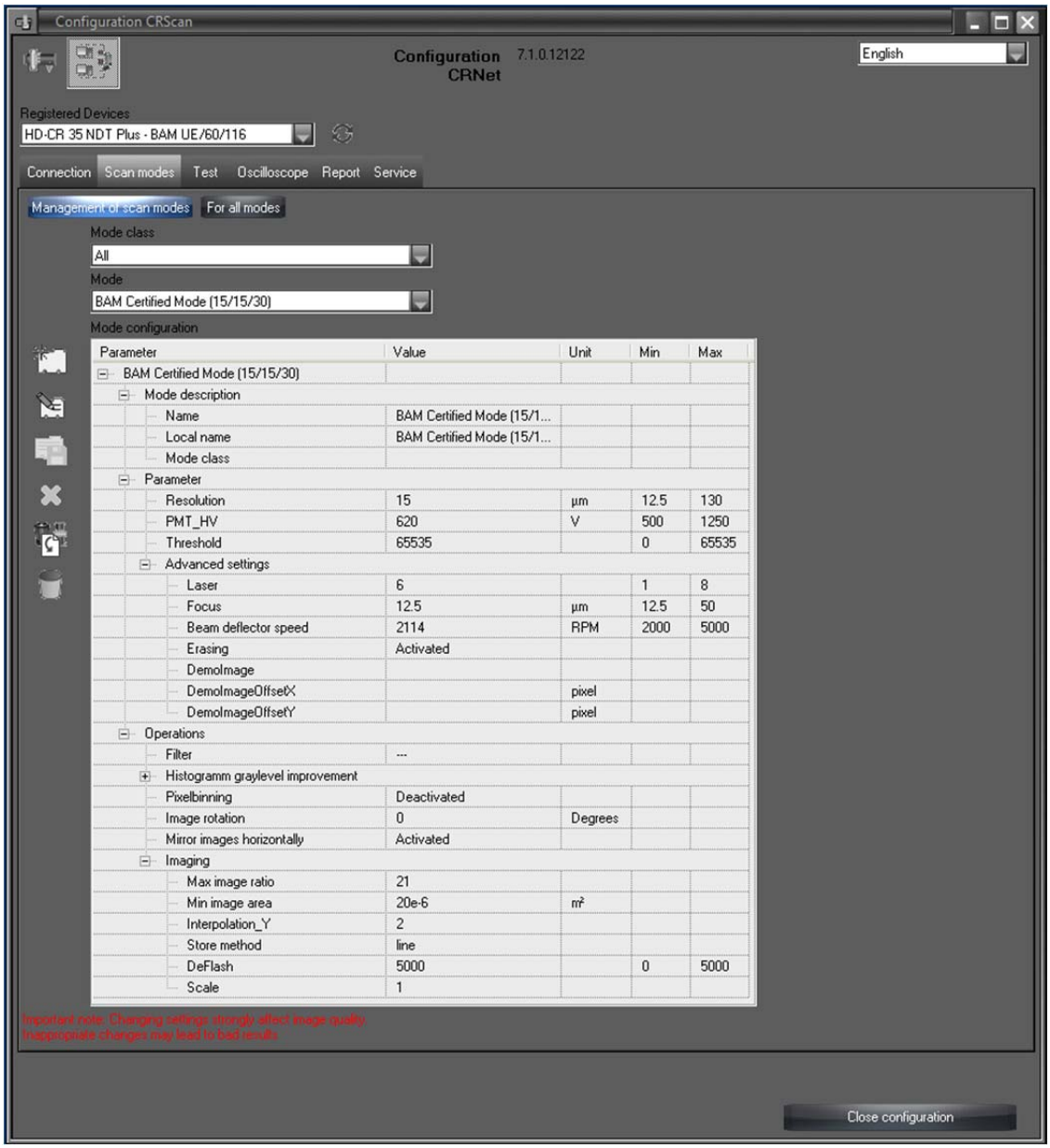

Fig. 1: Set-up of scanner device parameters used for system classification of the HD-CR 35 NDT Plus scanner, running the programme “Vistascanconfig.exe” and using the scan mode “BAM Certified mode (15/15/30)”

The set-up shown in fig. 1 is stored directly inside the scanner connected via Ethernet and NOT as configuration file “vistascan.ini” in the sub-dir “C:\Duerr\vistascan\” as for the older scanners connected by the USB interface.
The setting “Interpolation_Y = 2” ensures that the scanner scans with the double speed in slow-scan direction, which results in a rectangular pixel size of 15.5 µm (fast-scan) by 31 µm (slow-scan) during the scan. The device driver inside the scanner corrects this after scanning and duplicates all scan lines in the image. This increases the file by a factor of two, but provides again a quadratic pixel size and a correct aspect ratio for image viewing. In this way the scanning speed is doubled and the basic spatial resolution has the same values in fast-scan and slow-scan direction as shown in section 1.1.

All scans were performed with a pixel size setting of 15.5 µm and a high voltage setting of the photo multiplier (PMT) of 620 V. The laser power was reduced to 6 (from maximum 8) to reduce scanning artefacts. This allows a max. X-ray dose of 47 mGy for the saturation of the scanner (max. grey values clipped at 65 500) with HD-IP$^+$ IPs. If the PMT voltage is increased, this clipping point is reduced for lower dose values without changing the SNR_N in the data. If the PMT voltage is reduced below 500 V, additional fading artefacts are introduced in the image, which originates from residual electrons in the PMT from the previous digitized pixel value. PMT high voltage values below 500V should be avoided.
All exposures have been carried out with HD-IP$^+$s 10x24cm² in standard film plastic bags without lead screens. This deviation from EN 14784-1 was agreed with Dürr, because a Pb screen reduces the flexibility of the thin IP and generates very easily scratches on the surface of the IP. The step exposure method with 220 kV and 8 mm Cu pre-filter was used for SNR_N measurements and IP system classification.
To ensure consistent results comparing different IP's from the same batch, a waiting time of 10 min was kept between end of exposure and begin of scanning to avoid varying fading effects.
All images are shown in negative mode as film images in this report, i.e. a high grey value (high dose) is shown darker.

Description of test results

1. Determination of unsharpness

1.1 Duplex wire method

The image unsharpness was determined with 2 duplex wire image quality indicators (IQIs) according to DIN EN ISO 19232-5. They were placed directly on the HD-IP tilted by 2° to 5° perpendicular and parallel to the Laser scanning direction (fast scan in the scanner unit) and exposed at 90 kV and a distance between source (focal spot size of 1.5 mm according to EN 12543-2) and object of 1.80 m. Fig. 2 shows the results for 90 kV at the scanner pixel size of 15.5 µm. There was no difference observed for 220 kV X-ray voltage and 8 mm Cu filter for beam hardening besides a reduced contrast of the duplex wire IQIs. Therefore, only the results for 90 kV have been shown in fig. 2.

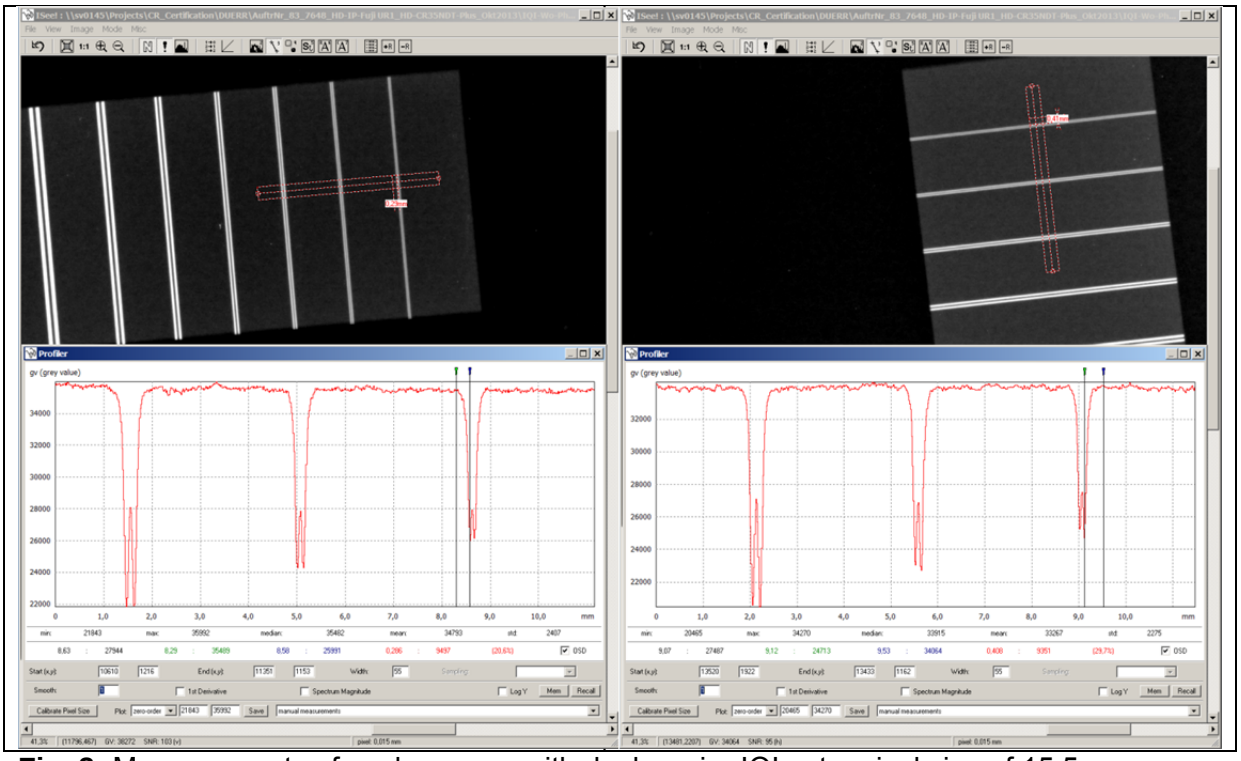

Fig. 2: Measurements of unsharpness with duplex wire IQIs at a pixel size of 15.5 µm.
Left side: Laser scan direction (fast scan), DD13 is resolved with > 20 % dip separation corresponding to a basic spatial resolution of 40 µm (see EN 14784-1; ">13D"), **Right side**:

slow scan direction, DD13 is resolved with > 20 % dip separation corresponding to a basic spatial resolution of 40 µm in slow scan direction. The maximum basic spatial resolution is SR_{max} = 40 µm.

The same basic spatial resolution was measured for the two spatial directions.
The maximum basic spatial resolution is the half of the larger unsharpness value (of both directions) rounded to the nearest 10 µm step. The investigated system HD-CR 35 NDT Plus scanner and HD-IP$^+$ imaging plate has the following maximum basic spatial resolution in the scanning mode shown in fig.1:

SR_{max} = 40 µm

1.2 MTF method

The unsharpness was measured also with the MTF method using a tungsten edge according to IEC 62220-1 at 90 kV X-ray voltage. In fig. 3 the results are shown for 15.5 µm scanner pixel size. An increase in X-ray energy or added lead front screens degrades the MTF further and lower the documented 20 % MTF values caused by additional scatter effects (low frequency drop of the MTF).
The SR_{max} values have to be taken from the measurements with the duplex wire IQIs (see fig. 2) according to EN 14784-1, so the MTF measurements are shown here for information only.

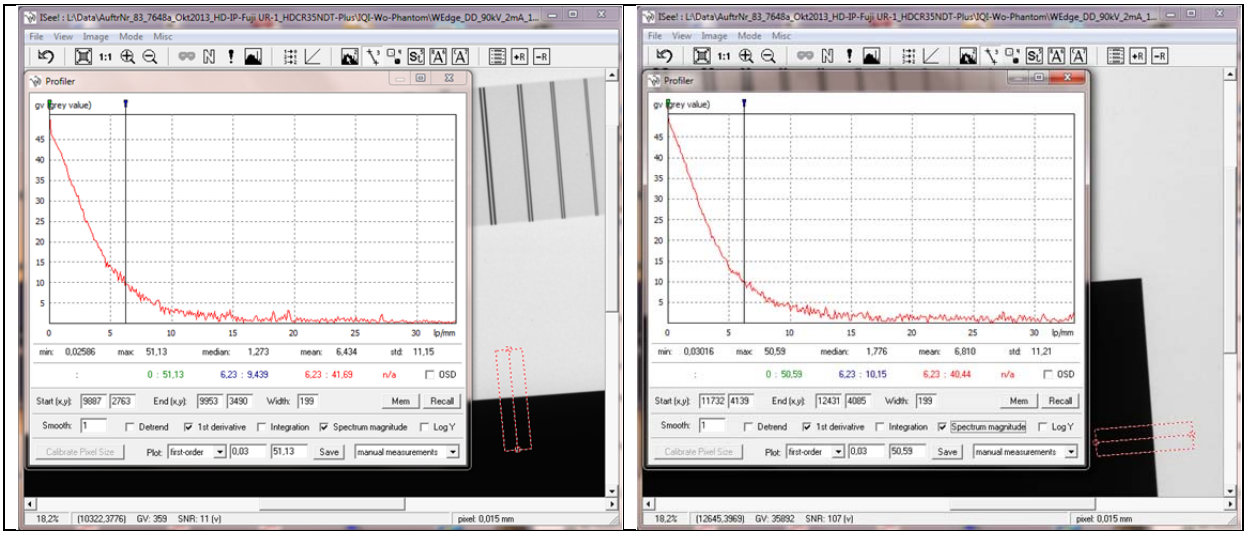

Fig. 3: MTF measurements at 90 kV, 15.5 µm nominal pixel size, **Left side:** slow scan direction, the 20 % MTF value is at 6.2 lp/mm (80 µm basic spatial resolution accord. to equation (4) in EN 14784-1), **Right side:** fast scan direction, the 20 % MTF value is at 6.2 lp/mm (80 µm basic spatial resolution accord. to equation (4) in EN 14784-1).

2. Measurement of the normalized Signal-to-Noise ratio (SNR_N)

The normalized SNR_N was measured according to the step exposure method (see 6.1.1 in EN 14784-1). The calibrated step exposure equipment available at BAM was used for these measurements. The same equipment is currently being used also for film system classification according to DIN EN ISO 11699-1. Compared to film exposures the step width was increased to 14 mm and the step distance to 24 mm with respect to the increased internal scattering observed with IPs as compared to film exposures. This increased step distance reduces the influence of the background from adjacent steps on the homogeneity of the exposed steps. The step height is unchanged (35 mm).

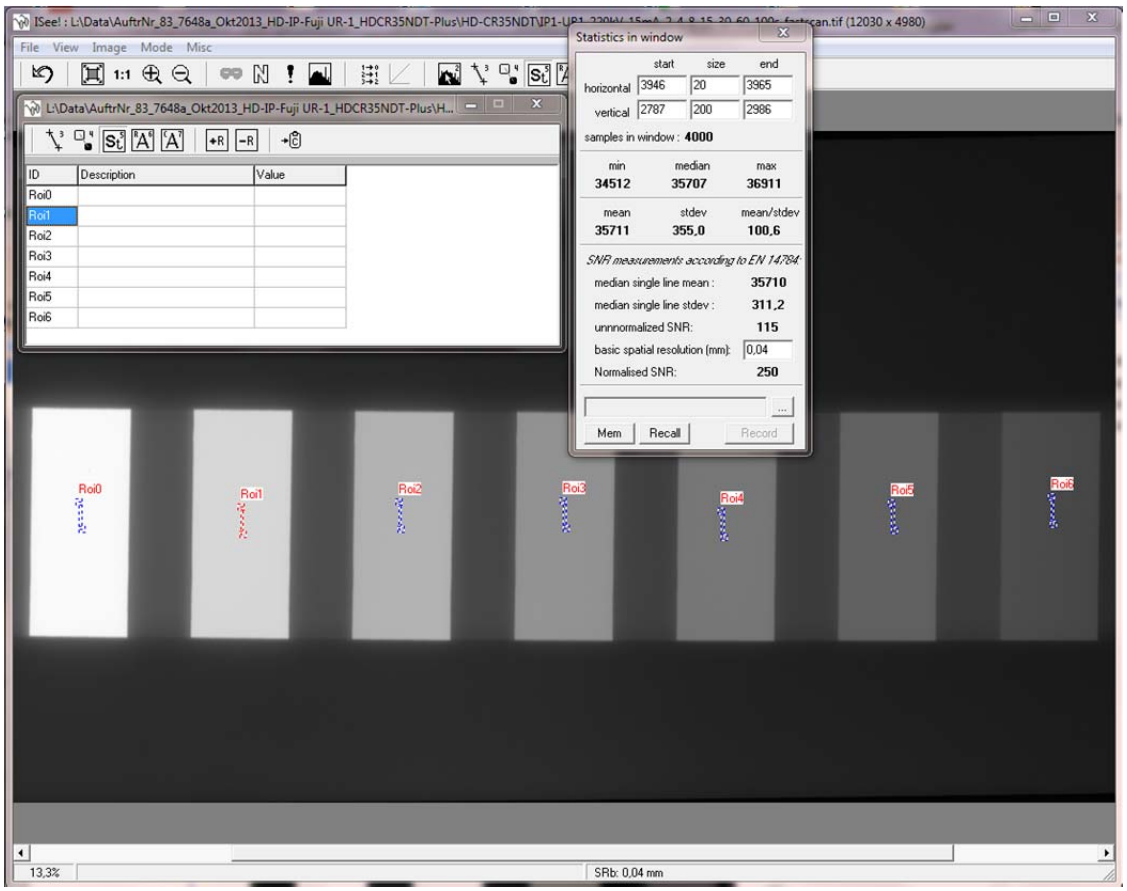

Fig. 4: Step exposure for SNR_N measurement. An image is shown with step exposures and marked regions for SNR_N measurements at the exposed steps. The ROIs are selected for SNR_N measurement in fast scan direction (i.e. IPs inserted into the scanner, that the fast scan direction is horizontal in this image).

The minimally required 12 different dose levels were obtained by 2 exposures with different exposure times and X-ray tube current settings. The corresponding dose for a step with a defined exposure time can be calculated on the basis of a dose calibration of 24.4 µGy/mAs at 220 kV and 8 mm Cu pre-filtering. A waiting time of 10 min was strictly kept between end of exposure and begin of scanning of the IP in the CR scanner to avoid derivations due to fading effects in the IP and thus to obtain reproducible results.

All SNR_N measurements have been done with a window size of 20 pixel width (20 values per group in horizontal direction) and 200 pixels height (i.e. 200 groups for median in vertical direction).

Because of equal unsharpness in slow and fast scan direction (see chapter 1), the directional measurement of SNR_N based on the median procedure in slow scan and fast scan direction will give equivalent values. After verification of this behaviour only the SNR measurements in fast scan direction are given in this test report. The SNR_N measurement tool of ISee! calculated the standard deviation for noise measurement for horizontal line groups, which are 20 pixels wide here (see fig. 4).

The measured relationship between dose and signal intensity (acquired raw grey values) is shown in figures 5 and 6. A linear relationship was observed, the tolerance in signal intensity at identical dose values was +/- 3 % for the 6 different imaging plates.

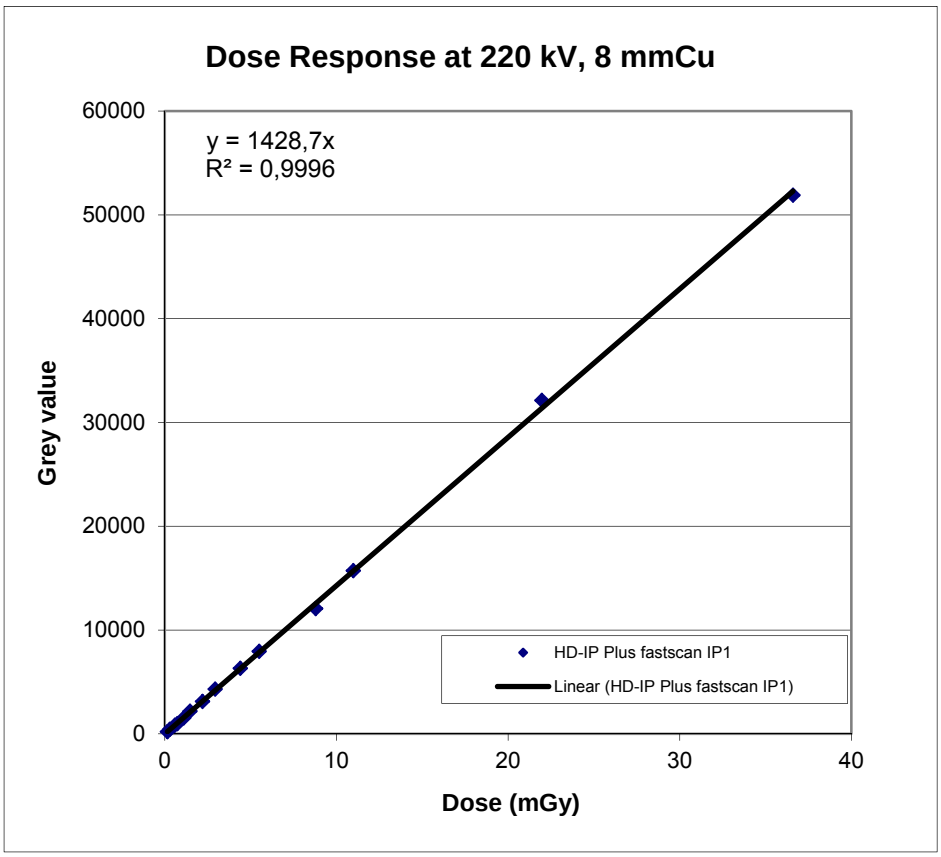

Fig. 5: Fit of grey values (linear signal intensities I_{meas}) versus exposure dose for a single imaging plate (no. 1) over 14 steps with different dose values at 15.5 µm pixel size read-out.

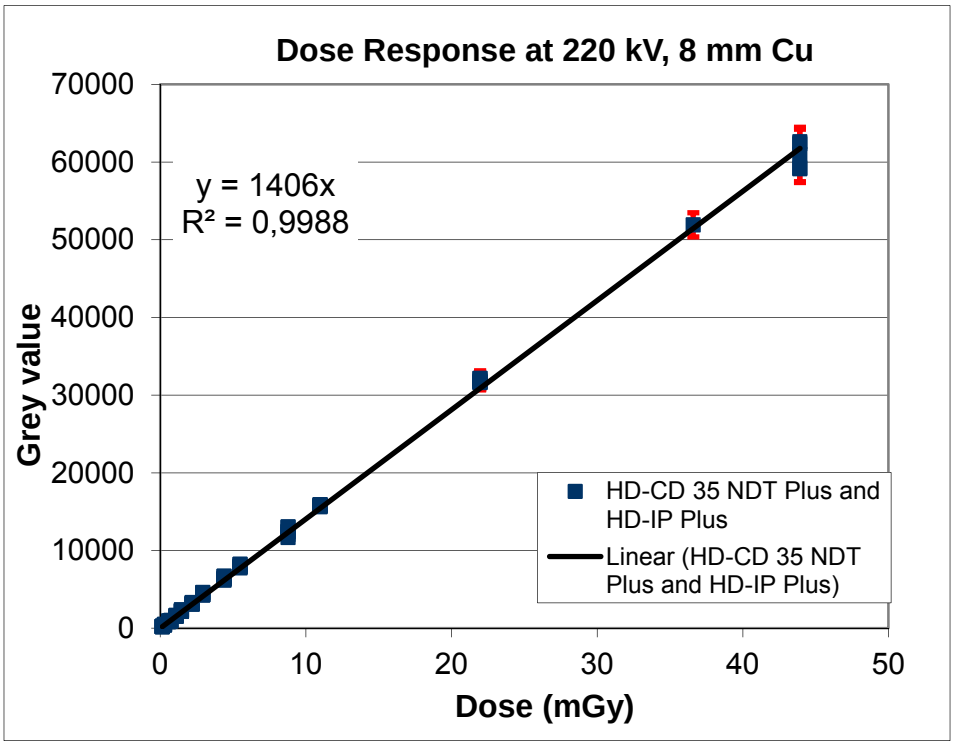

Fig. 6: Fit of dose response including all measurements of 6 different imaging plates of the same batch. The mean gain (slope) is 1406 grey values per mGy dose. The differences between individual plates are within a tolerance of +/- 3 % of the grey values. This is a result of slope variations between individual imaging plates (i.e. slope = 1429 / mGy for screen no. 1 and 1406 / mGy as mean slope over all 6 plates).

The measured normalized SNR_N in fast scan direction of all 6 imaging plates at the 14 different dose values in the range of 0.15 mGy up to 44 mGy is shown in fig. 7. An improved noise model was applied as compared with Annex A in EN 14784-1, in which the normalized SNR_N was fitted with a straight line in a semi-logarithmic graph. This improved noise model allows the analysis of the SNR_N for saturation by IP structure noise, which is typical for imaging plates. The standard deviation of the signal at SNR_N saturation is proportional to the radiation dose for structure noise and no longer proportional to the square root of the dose as for the quantum noise. The consecutive contributions for the standard deviation σ caused by signal noise are dependent on the radiation dose K as follows (summing up quadratically):

$$\sigma^2 = a + b\,K + c\,K^2 \qquad (3)$$

The constant a describes the dose-independent contribution (electronic read-out noise or signal differences between read-out lines), b refers to the quantum noise contribution (σ proportional to √K) and c is the noise contribution proportional to the dose (structure noise). The following model for the signal-to-noise ratio $SNR_N = I/\sigma$ is derived from a dose-proportional signal intensity (I_{meas} = Gain · K):

$$SNR_{model} = \frac{K}{\sqrt{a + bK + cK^2}} \qquad (4)$$

The maximum reachable $SNR_{N,max}$ limited by structure noise (saturation value), can be calculated as:

$$SNR_{N,\max} = \frac{1}{\sqrt{c}} \qquad (5)$$

The noise model in fig. 7 (red curve) has the following model parameters:

$a = 4.94 \cdot 10^{-5}$, $b = 3.61 \cdot 10^{-4}$, $c = 8.20 \cdot 10^{-6}$, with $\mathbf{SNR_{N,\,max} = 349}$ (6)

The electronic read-out noise can be neglected for this CR system. The maximum $SNR_{N,max}$ achievable with the tested CR system is 349. The error bars shown in fig. 7 represent a tolerance of +/-3 % of the measured SNR_N values. This tolerance describes the differences between all 6 investigated imaging plates as well as the deviation between the simple model of EN 14784-1 (line “Logarithmisch (Model)” in the semi-logarithmic plot of fig. 7) and the model according to equation (4) within the SNR_N range of 43 and 130. For this reason the formula given in fig. 7 was used to determine the minimum dose values for all CR system classes in accordance with Annex A in EN 14784-1. From a given minimum signal-to-noise ratio SNR_{IPx} of the CR system class IPx the corresponding minimum dose $K_{S,IPx}$ was calculated according to equation (7) (inversion of the formula in fig. 7):

$$K_{S,IPx} = \exp((1.03 \cdot SNR_{IPx} - 49.473)/38.439) \qquad (7)$$

The factor of 1.03 in equation (7) takes into account the measurement tolerance of +/-3 % of SNR_N, resulting from the deviations between the different imaging plates. Therefore, the necessary minimum dose was $1.03 \cdot SNR_{IPx}$.

Table 1 summarizes the results for all 6 IP system classes, the CEN speeds derived from the minimum dose values (see 7.3 in EN 14784-1) and the minimum linear signal intensities I_{IPx} according to equation (8):

$$I_{IPX} = 1.03 \cdot 1406 \cdot K_{S\,IPx} = 1448 \cdot K_{S\,IPx} \qquad (8)$$

The correction factor of 1.03 accounts for the tolerance of +/-3 % of the individual gain variation for the different imaging plates of the same batch (see fig. 6), whereas a tolerance of +/-3 % was already derived from the SNR_N measurements in equation (7).

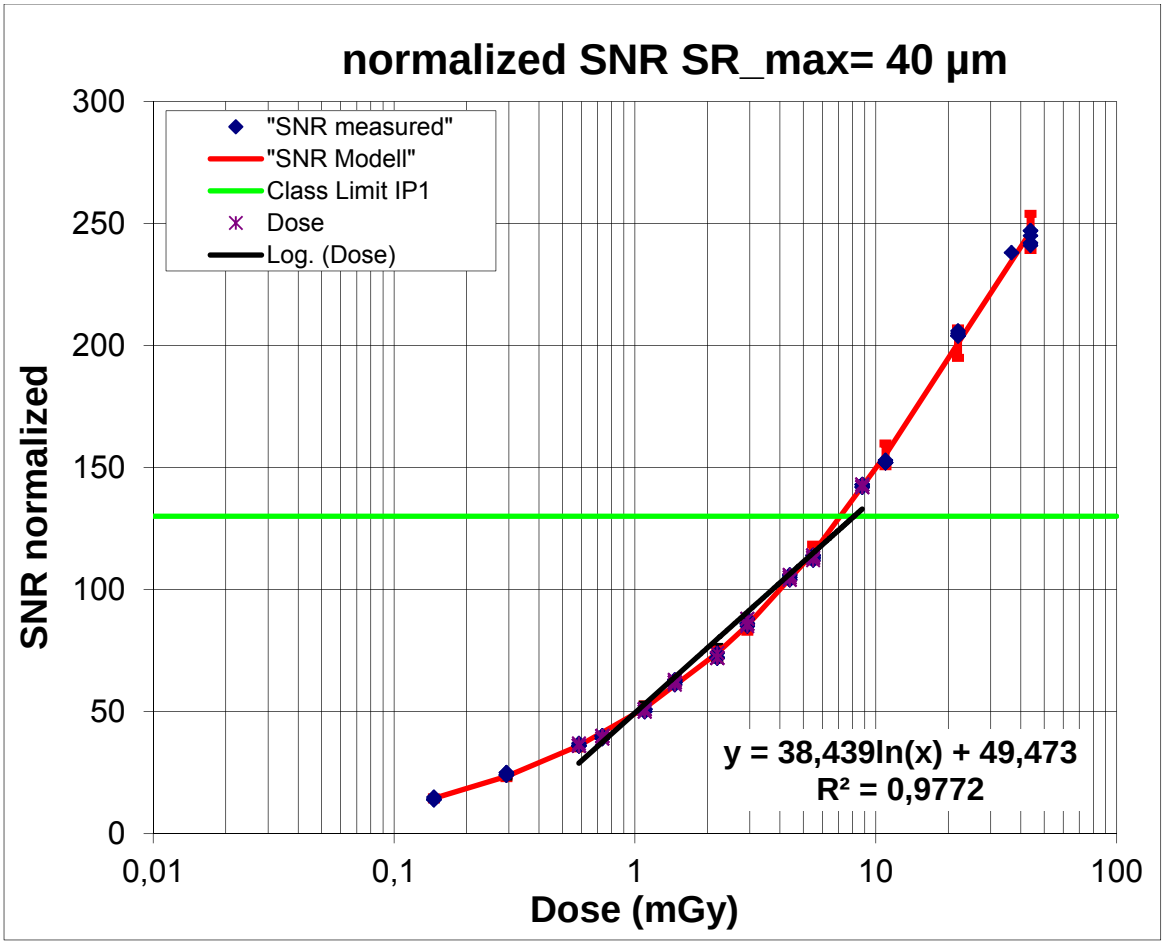

Fig. 7: Semi-logarithmic plot of the normalized SNR_N measurements in fast scan direction of 6 imaging plates at 14 dose values considering the noise model according to equations (4) and (6) as well as the logarithmic fit according to Annex A in EN 14784-1. The error bars represent a tolerance of +/-3 % of the SNR_N values. The green line corresponds to the minimum value of SNR_N = 130 of the highest IP system class IP1 mentioned in the certificate.

ASTM system class	CEN system class	minimum normalized SNR_{IPx}	minimum dose K_S / mGy	CEN / ISO speed $S_{CEN} = S_{ISO}$	minimum linearized intensity I_{IPx}
IP special / 40	IP1/40	130	8,99	100	13050
	IP2/40	117	6,35	160	9200
	IP3/40	78	2,23	500	3250
IP I / 40	IP4/40	65	1,58	640	2300
IP II / 40	IP5/40	52	1,11	1000	1650
IP III / 40	IP6/40	43	0,87	1250	1300

Table 1: CR system classification for the HD-CR 35 NDT Plus scanner and HD-IP$^+$ imaging plates in fast scan direction (pixel size: 15.5 µm, PMT_HV = 620V). Film plastic bags have been used for exposure without lead screens.

The semi-logarithmic plot in fig. 7 shows only minor signs of the saturation effect for high dose values by the structure noise of the imaging plates. This is visualized by a plot of SNR_N versus square root of dose (see fig. 8). In this representation a nearly straight line fits to the low dose range, where the SNR_N is dominated by quantum noise, which is directly proportional to the square root of the dose. For dose values above 7 mGy the structure noise becomes more and more dominant, which results in the saturation of SNR_N at $SNR_{N,max}$= 349

for high dose values (above 100 mGy). This saturation value depends mainly on the type of imaging plate and limits the contrast sensitivity for high dose values.

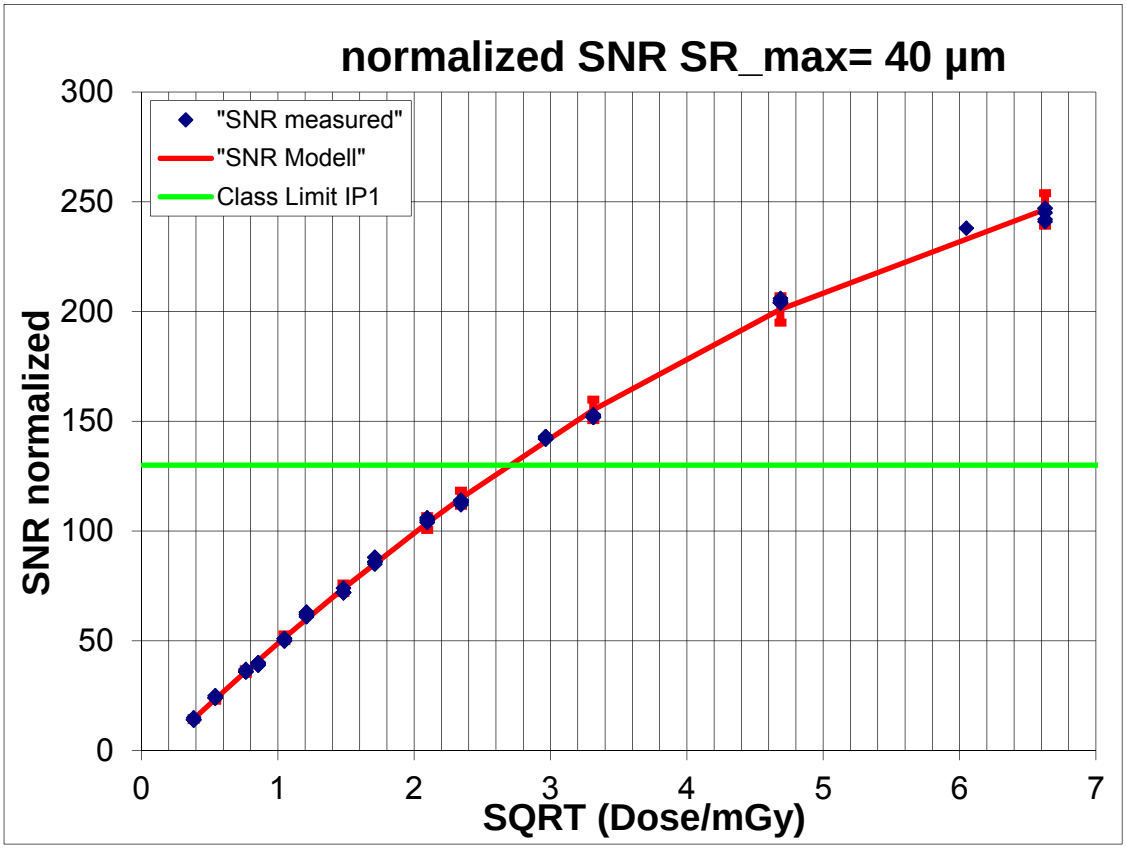

Fig. 8: Plot of the normalized SNR_N measurements in fast scan direction versus square root of dose of 6 imaging plates HD-IP$^+$ at 14 dose values following the noise model according to equation (4) and (6). The error bars show a tolerance of +/-3 % of the SNR_N values. The saturation effect of SNR_N by structure noise at high dose values ($SNR_{N.max}$=349) becomes more evident in this presentation.

The investigated scanner test sample showed no differences between fast and slow scan direction for SR_b, SNR and normalized SNR_N.

3. Other tests with the CR test phantom

The CR test phantom was radiographed at 90 kV and a source distance of 1.8 m directly above an HD-IP$^+$ without Pb screens. An overview image is shown in fig. 9.

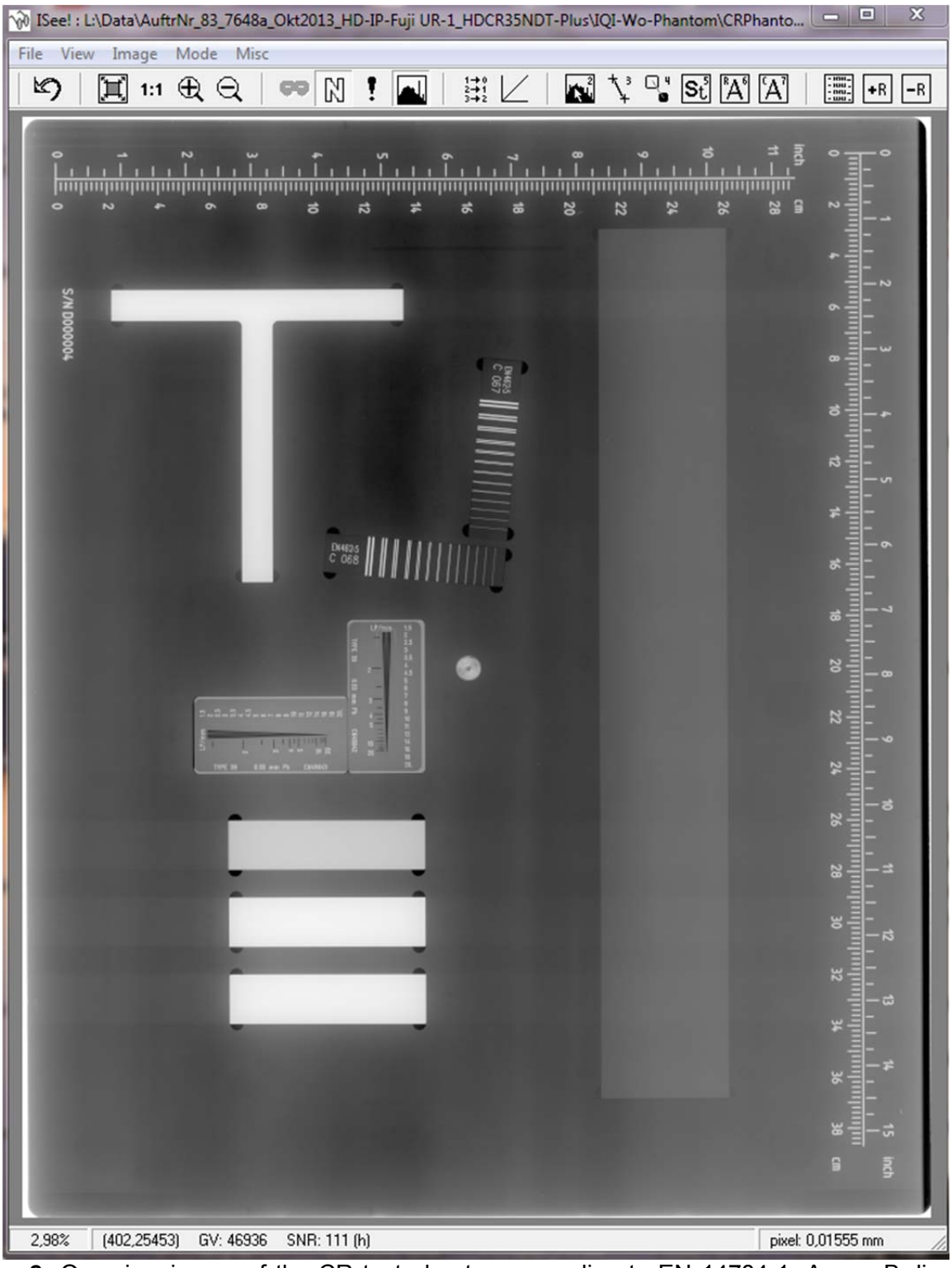

Fig. 9: Overview image of the CR test phantom according to EN 14784-1, Annex B, linear signal intensity in the background near to BAM snail is 58700, SNR_N = 240 in fast scan direction, exposure at 90 kV, 240 mAs, SDD=1800 mm, IP without Pb screens in plastic bag.

3.1. Geometric distortions

The spatial linearity and the exact pixel sizes has been determined separately for the fast scan and slow scan direction by means of the spatial linearity quality indicators built-in into the CR test phantom. Fig. 10 shows the measurement results. The maximum deviation from the nominal size of 15.50 µm is 15.49 µm in slow scan direction. This deviation in relative pixel size is <0.1 % and far below the allowed limit of +/-2 %. This test passed successfully.

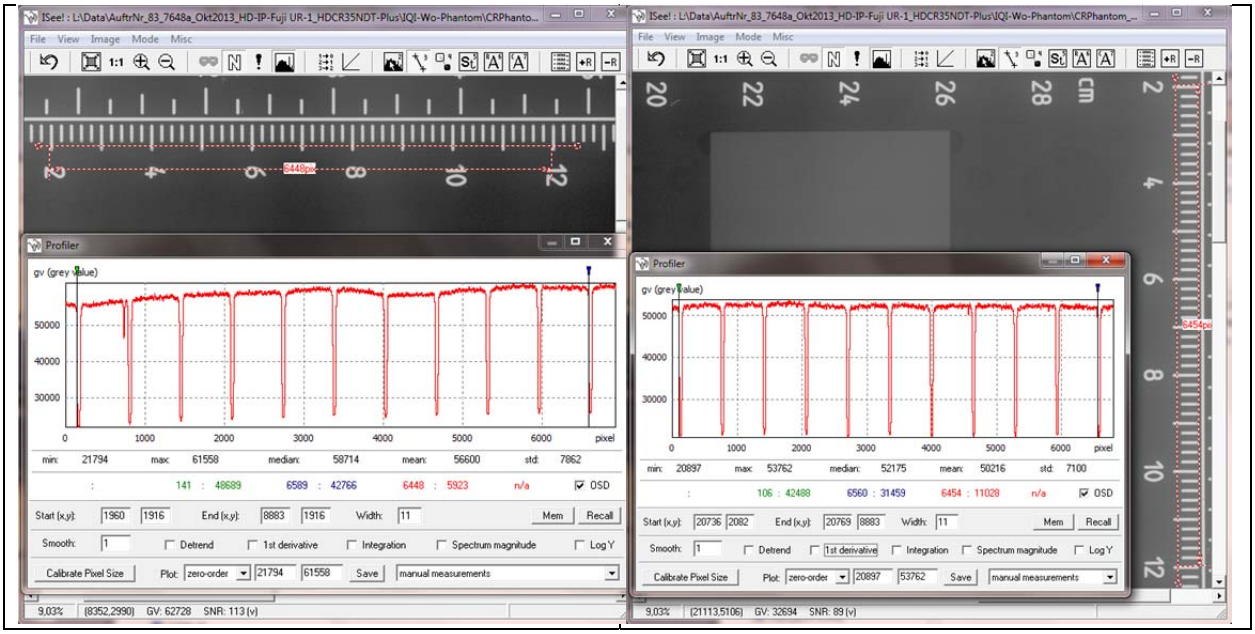

Fig. 10: Measurement results for the horizontal pixel size (100mm/6448= 15.50 µm) in fast scan direction (left hand side) and the vertical pixel size (100mm/6454= 15.49 µm) in slow scan direction (right hand side).

3.2 Laser beam function

The Laser beam function was evaluated by the edge response of the high-absorbing T-target of the CR test phantom (see fig. 11).
At a 5x pixel magnification under- or overshoot within and between the scan lines at the edge should be detectable in case of Laser malfunction. The scan result shown in fig. 11 does not show any problem, this test passed successfully.

3.3 Blooming or flare

The scanning system shows flare or blooming contributions < 3.5 % contrast in the fast scan direction (see fig. 12). No blooming or flare has been observed in slow scan direction. This test passed successfully.

3.4 Scanner slipping

Scanner slipping and background non-uniformity are evaluated with the help of test target G (homogeneous strip of Al, 0.5 mm thick) in the CR test phantom. The power spectrum of the profile across the Al strip in slow scan direction (see profiler in fig.13) does not indicate any special frequency arising from the transport mechanism as it was observed with previous scanner models. This test passed too.

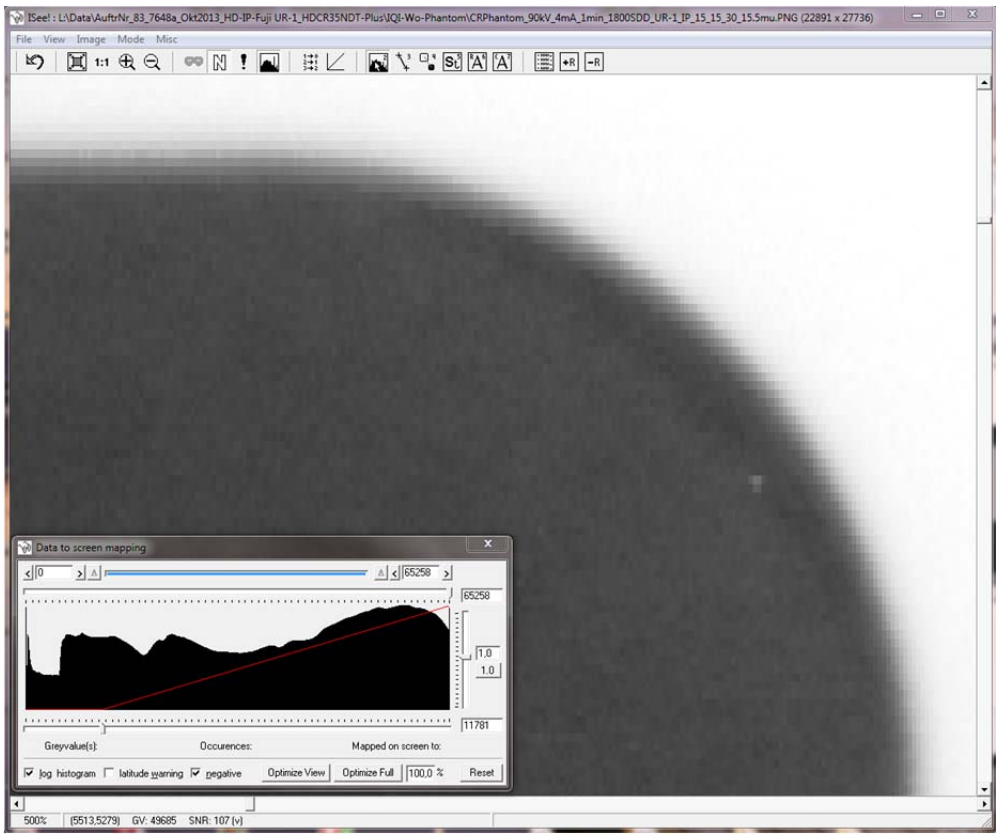

Fig. 11: Test of Laser beam function at the edge of the T-target in the CR test phantom.

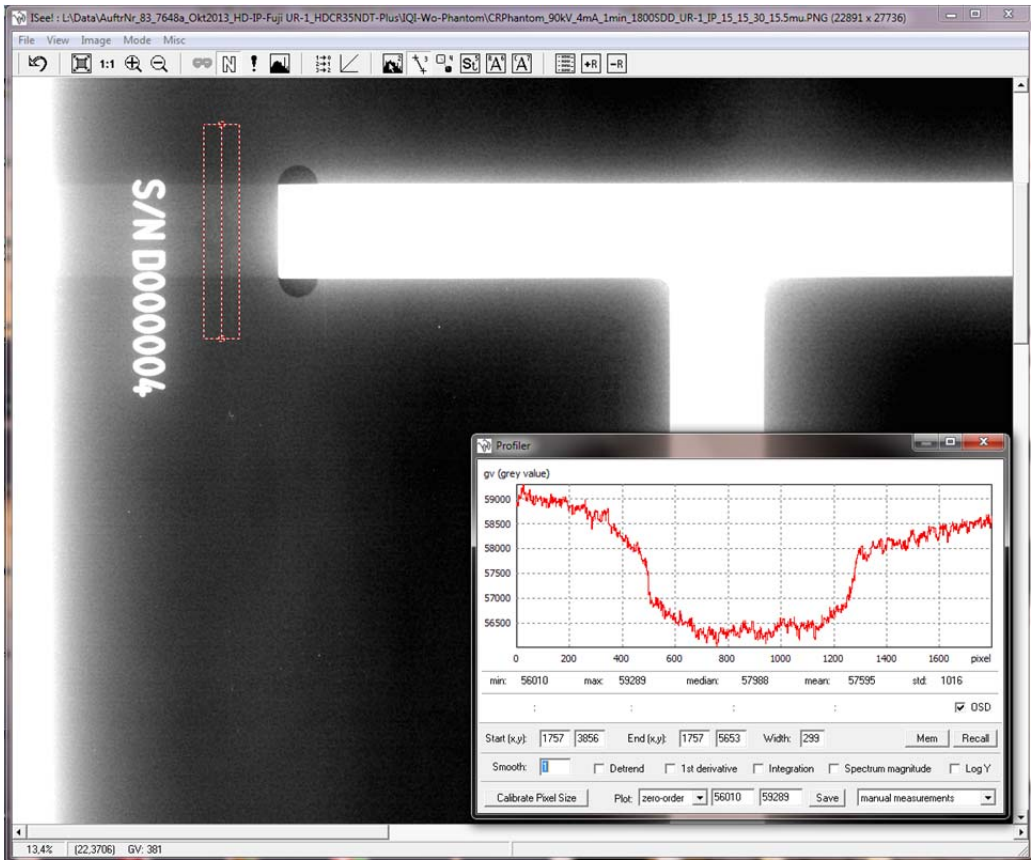

Fig. 12: Test of blooming or flare at the T-Target. The relative flare contribution in fast scan direction at the profile position shown directly at the end of the T-target is below 3.5 %.

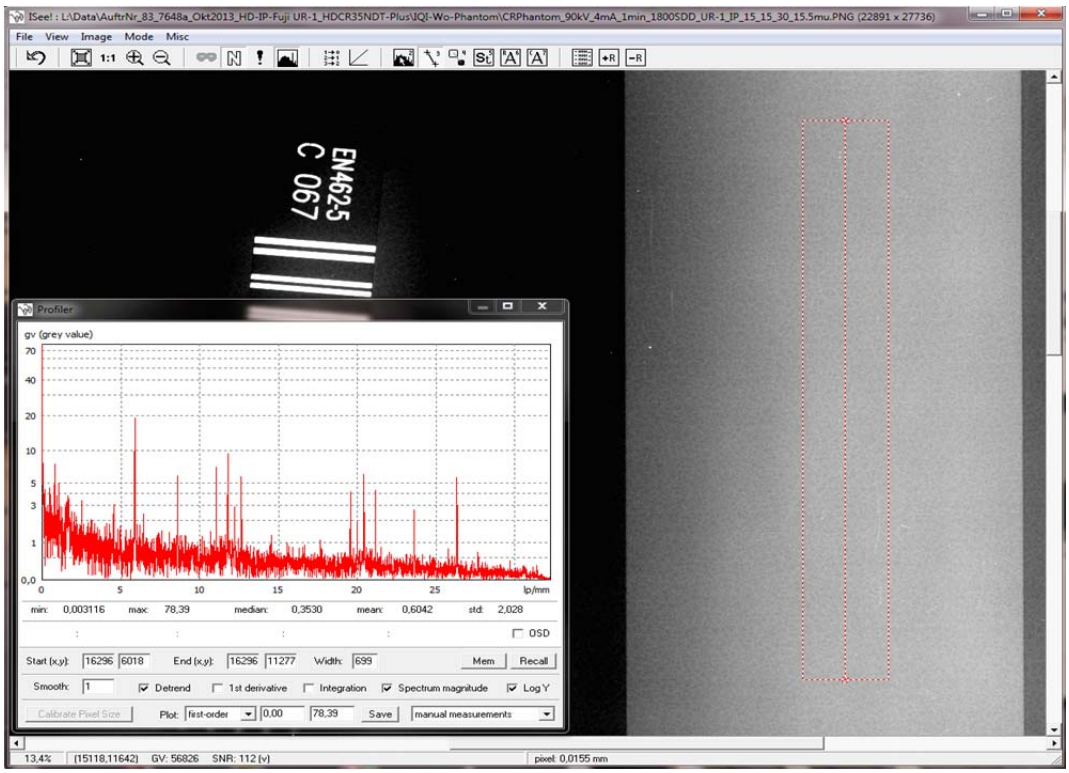

Fig. 13: Evaluation of scanner slipping and background non-uniformity. No artefacts are visible in this image as well as in the power spectrum of a profile in slow scan direction across the Al strip.

3.5 Shading

The integrated profile in fig. 14 shows horizontal shading in the image background of ca. +/- 7 % originated from the IP transport mechanism of the scanner, whereas a signal intensity variation of 14 % is observed between the shading quality indicators (the Lucite holes EL, EC and ER in the CR test phantom).

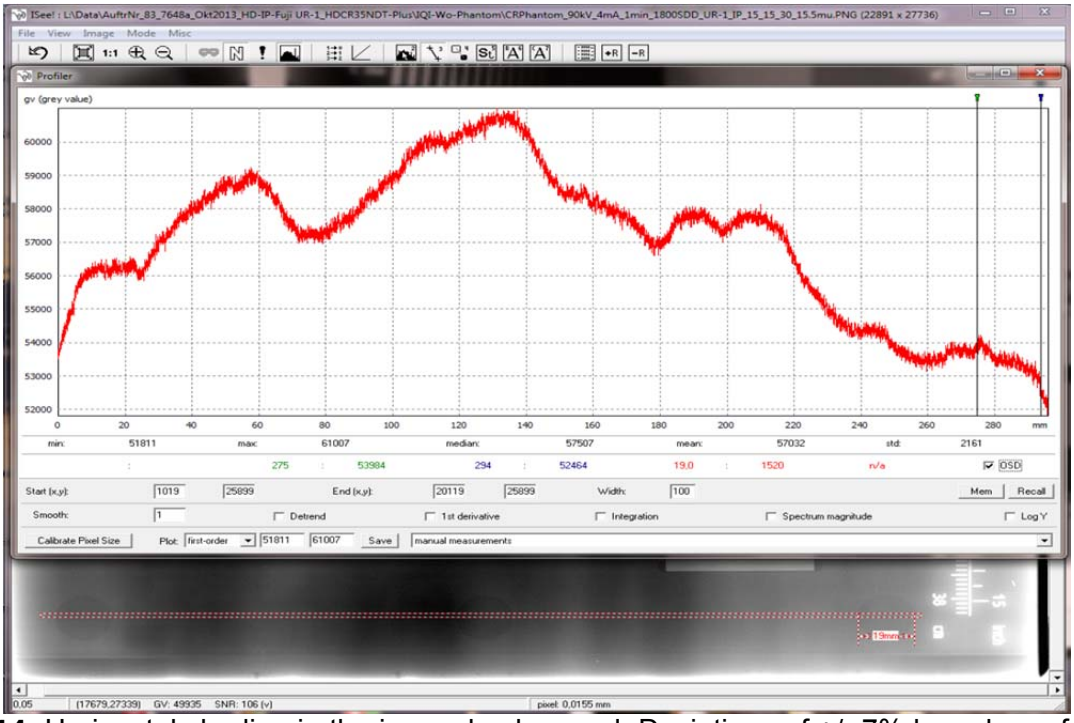

Fig. 14: Horizontal shading in the image background. Deviations of +/- 7% have been found, generated by the IP transport system in the scanner. The shading between the holes ER, EC, EL is 14 % (gv_{min} = 53 000, gv_{max} = 61 000).

Additionally, the observed overall background shading is amplified by the dose variation of the X-ray tube depending on the opening angle too.
The maximum allowed shading is +/- 10 % according to EN 14784-1, so this test passed too.

3.6. Erasure of imaging plates

The scanner has a built-in erasure unit, the erasure time is identical with the scanning time. The scanning time depends on the pixel size, for larger pixel sizes the scanning and erasure time is shorter. For the scan mode used here (see fig.1) the erasure speed was 65.5 mm/min. A scan directly after erasure results always in grey values below 50 and did not show any residual structures. An overall average grey value below 10 confirmed that the minimum signal intensity after external erasure is below 1 % of the maximum signal intensity of the previous exposed image (limit in EN 14784-1). The test passed.
For higher energies and larger pixel sizes (resulting in a higher erasure speed too) it may be necessary to longer erasure times.

3.7. Summary of tests based on the CR test phantom

All tests according to EN 14784-1 performed with the CR test phantom passed. The results can be summarized according to Annex C.3 in EN 14784-1 as follows:

a) basic spatial resolution in fast scan direction: 40 µm, in slow scan direction: 40 µm, measured real pixel size: 15.5 µm
b) recognized contrast sensitivity on IQIs according to ASTM E 1647-98a:
Al: <1 %, Cu > 4% and SS: >4 %
c) slipping: no
d) jitter: no
e) max. background shading of raw data: +/- 7% at 1.80 m source object distance, overall shading of 5% by X-ray radiation, shading between the holes EL, EC, ER is 14%
f) radiation parameters: 90 kV, 4 mAmin, 1.80 m distance, HD-IP$^+$ without Pb screens, linear signal intensity in background near to BAM snail is 58 700, SNR_N = 240 in fast scan direction, scanning at 15.5 µm pixel size
g) performed on December 8th 2013 by Dr. Uwe Zscherpel

Note

This test report refers only to EN 14784-1 or ISO 16371-1 (identical text). The requirements according to ASTM E 2445 and E 2446 are analogue, but differently structured. For readability and simplicity reasons the references to the ASTM standards have been omitted in the text.

BAM Federal Institute for Materials Research and Testing
Division 8.3 "Nondestructive Testing - Radiological Methods"
D-12200 Berlin, 2014-05-06

on behalf

Prof. Dr. Uwe Ewert
Head of Division 8.3

on behalf

Dr. Uwe Zscherpel
Person in charge